Fluorescence Spectroscopy, Exciton Dynamics, and Photochemistry of Single Allophycocyanin Trimers

Liming Ying[†] and X. Sunney Xie*

Pacific Northwest National Laboratory, William R. Wiley Environmental Molecular Sciences Laboratory, P.O. Box 999, K8-88, Richland, Washington 99352

Received: July 30, 1998; In Final Form: October 14, 1998

We report a study of the allophycocyanin trimer (APC), a light-harvesting protein complex from cyanobacteria, by room-temperature single-molecule measurements of fluorescence spectra, lifetimes, intensity trajectories, and polarization modulation. Emission spectra of individual APC trimers are found to be homogeneous on the time scale of seconds. In contrast, their emission lifetimes are found to be widely distributed because of generation of long-lived exciton traps during the course of measurements. The intensity trajectories and polarization modulation experiments indicate reversible exciton trap formation within the three quasi-independent pairs of strong interacting α84 and β84 chromophores in APC, as well as photobleaching of individual chromophores. Comparison experiments under continuous-wave and pulsed excitation reveal a two-photon mechanism for generating exciton traps and/or photobleaching, which involves exciton−exciton annihilation. These single-molecule experiments provide new insights into the spectroscopy, exciton dynamics, and photochemistry of light-harvesting complexes.

Introduction

Recent advances in fluorescence microscopy and spectroscopy at room temperature have made it possible not only to detect, image and conduct spectroscopic studies of single fluorophores, but also to monitor the dynamic processes of individual biological macromolecules.[1−18] While conventional experiments probe the averaged behavior of large ensembles of molecules, single-molecule measurements allow distribution of molecular properties to be determined. Moreover, real-time measurements of single-molecule trajectories allow dynamic information to be interrogated at a level of great detail. Single-molecule studies have been carried out for both spontaneous and photoinduced dynamical processes. We will mostly focus on the photoinduced phenomena in this work.

One of the interesting applications of single-molecule spectroscopy is the study of the exciton dynamics of molecular aggregates, which have been explored by a few groups.[12,17−19] Weiss and co-workers demonstrated the fluorescence measurement of a single donor−acceptor pair separated by a DNA duplex.[12] Sequential photobleaching of the donor and acceptor were experimentally observed. In a flow cytometry experiment, Wu et al. made an interesting observation on B-phycoerythrin, a light-harvesting phycobiliprotein containing a cluster of 34 bilin chromophores.[19] They found that the photobleaching of a single B-phycoerythrin molecule occurs in a single step. With confocal microscopy, two detailed studies of the single light-harvesting complex LH2 from *Rhodopseudomonas acidophila* and single conjugated polymers have been carried out recently by Hochstrasser and co-workers[17] and by Barbara and co-workers,[18,20] respectively. Both groups showed that, in addition to one-step bleaching, single aggregate emission can be switched between on and off states by the formation of exciton traps, which quench the fluorescence during the emission off-time. The emission on-times were linearly dependent on excitation intensity, suggesting a photoinduced mechanism for the generation of exciton traps. The off-times were independent of excitation intensity, suggesting a spontaneous recovery. The exact chemical nature and mechanism of formation for the exciton traps are not yet known. In the case of light-harvesting complex LH2, it was suggested that radical cations of bacteriochlorophyll *a* are formed via photoinduced electron transfer.[17] Here we report a series of single-molecule experiments done on allophycocyanin (APC), a simpler and well-characterized molecular aggregate. The motivation of this work is to reveal the underlying mechanisms for the photochemistry and photophysics of single APC trimers.

Allophycocyanin is located at the core of the phycobilisome, a light-harvesting apparatus in cyanobacteria.[21] Together with other phycobiliproteins, such as phycocyanin and phycoerythrin, APC is responsible for efficient capturing and funneling electronic excitation to the membrane-bound photosynthetic reaction centers (PS II) where fast electron transfer occurs with high efficiency, converting solar energy to chemical energy. The crystal structure of the APC trimer from *Spirulina platensis* has been solved recently by Huber and co-workers.[22] A schematic representation of the structure is shown in Figure 1A. Three αβ monomers are arranged around a 3-fold symmetry axis to form a trimer $(\alpha\beta)_3$ which has a diameter of approximately 11 nm, a thickness of 3 nm, and a central channel 3.5 nm in diameter. In each monomer, an α or a β polypeptide chain covalently binds a phycocyanobilin (open-chain tetrapyrrole) chromophore through a cystein residue α84 or β84. Upon aggregation to a trimer, the α84 chromophore in one monomer is brought close to the β84 chromophore in an adjacent monomer, forming a strongly interacting pair with a center-to-

[†] Current address: College of Chemistry and Molecular Engineering, Peking University, Beijing 100871, P.R. China.

* To whom correspondence should be addressed.

10.1021/jp983227d CCC: $15.00
Published on Web 11/24/1998

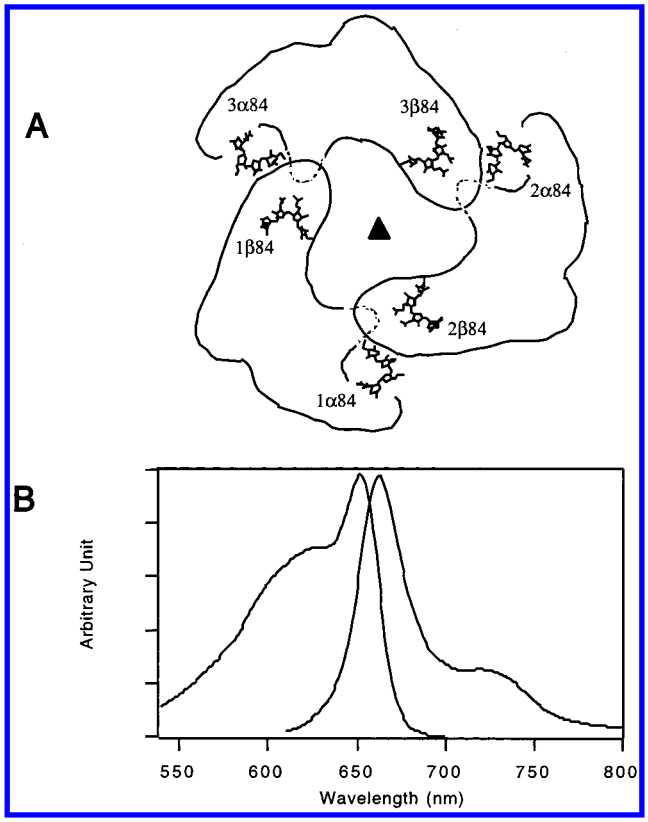

Figure 1. (A) Schematic representation of allophycocyanin trimer based on the X-ray crystal structure determined by Huber and co-workers.[22] The α84 and *β*84 phycocyanobilin choromophores are shown. (B) Absorption (left) and emission (right) spectra of cross-linked allophycocyanin trimers in pH 7.4 buffer solution.

center distance of 2 nm. The absorption spectrum of APC trimer is significantly different from that of the monomer, with a red-shifted sharp peak at 654 nm (Figure 1B).

There are two limiting cases of excitonic interaction for a donor and acceptor pair. In the strong coupling limit, the strong dipole−dipole interaction results in a visible splitting in the absorption spectrum and the two excitonic states are delocalized within the entire molecular complex.[23] In the weak coupling limit, the dipole−dipole interaction between the chromophores does not significantly alter the absorption spectrum and incoherent energy transfer is adequately described by Förster theory.[24] The interaction between α84 and *β*84 within a pair falls in the intermediate-to-strong coupling range. Steady-state spectroscopic measurement of APC, circular dichroism in particular,[25,26] as well as recent femtosecond pump−probe measurements[27,28] have indicated that the 654 nm peak is the lower excitonic band and 623 nm peak is the higher excitonic band. On the other hand, interactions between chromophores in different pairs fall in the weak coupling limit. There have been extensive time-resolved studies characterizing excitonic interactions within the pairs of strongly interacting α84 and *β*84 chromophores, as well as energy transfer between the weakly interacting pairs.[29,30] The fact that the APC trimer has both strong and weak coupling in the multichromophore system makes it particularly suitable for single-molecule spectroscopic studies of exciton dynamics.

A central issue in the spectroscopy of biological systems is spectral heterogeneity, which arises from different local environments of chromophores. The fluctuation of the local environment takes place on a time scale ranging from femtoseconds to seconds. The time resolution of single-molecule trajectory measurements is on the order of a millisecond. Single-molecule experiments are capable of probing static heterogeneity and fluctuations slower than milliseconds. For single-dye molecules in polymers, spectral heterogeneity and spectral diffusion on the second time scale have been studied at room temperature.[14] The phenomenon was otherwise hidden in ensemble-average results. It is intriguing to probe spectral heterogeneity and fluctuations, if any, of a multichromophore system within a protein with the single-molecule experiments.

From a practical perspective, allophycocyanin is used as a fluorescent marker in immunoassay, flow cytometry, and fluorescence microscopy because of its large absorption coefficient, 7.0×10^5 cm^{-1} M^{-1}, and high quantum yield, 0.68-(31). In these applications, an intense focused laser beam is usually used to excite the fluorophores; the photophysical changes and photochemical damage are one of the important yet least understood aspects in the use of fluorescent labeling in life science research.[32] In demonstrating near-field fluorescence imaging of single protein molecules,[33] we found single APC trimers are more prone to photodamage than single chromophores under the high excitation intensity used. The experiments presented in this work shed light on various mechanisms for blinking and bleaching of multichromophore systems.

Here we report a series of single-molecule experiments on APC. Trajectories of the fluorescent intensity, spectra, and lifetimes have been recorded. While polarization modulation has provided valuable information on single molecule orientation and rotational motion,[4,34,35] we take advantage of the 3-fold symmetry of the APC trimer and use polarization modulation to probe the trap formation within the complex. Comparison of experiments under continuous-wave and pulsed excitation was also done to provide clues for the mechanisms of trap formation. The combination of single-molecule experiments led to new insights into exciton dynamics in the light-harvesting complex.

Experimental Section

Sample Preparation. Crossed-linked allophycocyanin trimers from *Anabaena variabilis* were supplied by Molecular Probes (Cat No. A-819). APC trimers were dialyzed in 0.1 M sodium phosphate buffer at pH 7.4 at 4 °C. Unlike normal APC trimers, cross-linked APC can exist in very dilute solution without disrupting the trimer structure.[36] The concentration of dialyzed solution was 1 mM, determined by its absorption spectrum. The sample was stored at 4 °C for daily use. This solution was further diluted by a factor of 10^4 with 0.1 M buffer prior to immobilization. We used two different approaches for immobilization. The first was agarose gel. One percent agarose (Sigma, Type VII) in 0.1 M phosphate buffer was kept above the geling temperature (40 °C) in a water bath. Two glass cover slips (Fisher Scientific) were first spin-coated with a very thin film (1−2 *μ*m) of the agarose gel. One microliter of the diluted APC solution was mixed with 20 *μ*L of gel solution. The two coated glass cover slips were used to sandwich a drop of the solution. After gelling in a few minutes, APC trimers were immobilized in the polymer matrix. The typical thickness of the gel was between 5 and 20 *μ*m. Single-molecule emission spectra indicated that the integrity of the APC trimers was maintained. Polarization modulation experiments (see below) indicated that most of the APC trimers did not undergo rotational diffusion in the gel. The second method for immobilization was by electrostatic interaction between the APC trimer and the charged glass surface. After incubation with a 50 *μ*L APC buffer solution for a few minutes, the glass cover slip was rinsed with buffer solution. The optical measurements were then conducted under the buffer solution. Both atomic force microscopy images and polarization measurements indicated that most of the disklike APC trimers were laid-

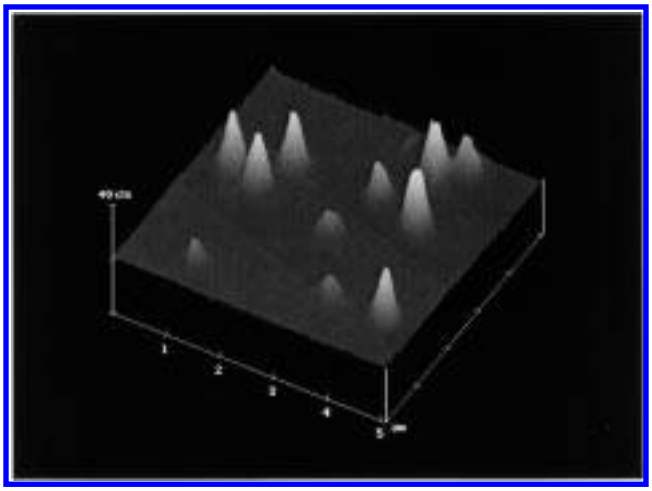

Figure 2. Fluorescence image of single allophycocyanin trimers taken in a 5 μm × 5 μm field. The molecules were immobilized on cover glass surface immersed under 0.1 M sodium phosphate buffer. The excitation wavelength was 568 nm, and laser irradiation power at the sample was 500 nW. Each peak is attributed to a single APC trimer.

down flat on the glass surface. We found no difference in the fluorescence spectra and lifetimes of the single trimers with these two kinds of sample preparations. This indicated that immobilization on the glass substrate does not perturb the spectroscopy of APC trimers. Most of the data presented below were taken in this manner.

Single-Molecule Fluorescence Measurements. The spectroscopic measurement was performed using a modified inverted fluorescence microscope (Nikon Diaphot).[14,15] The sample could be raster scanned or moved to a particular position using an *XY* stage (Queensgate). The excitation laser beam was intensity stabilized by a laser stabilization accessory (Liconix 50SA) and was attenuated to 200−700 nW. The excitation light was focused by a 60 × oil immersion objective (Nikon, numeric aperture 1.4), and the emission was collected by the same objective. The excitation light was blocked by a dichroic mirror and colored glass filters; fluorescence was detected by a photocounting avalanche photodiode (EG&G Canada, SPCM-200) at the focal plane of the camera port. Figure 2 shows a 5 μm × 5 μm fluorescence image of APC trimers adsorbed on a glass surface and immersed under a buffer solution. Each peak is attributed to a single APC trimer.

For measurements of single-molecule spectra, the 568 nm line from an Ar−Kr ion laser (Melles Griot, 643-AP-A01) was used as the excitation source. Fluorescence spectra of single APC trimers were measured by a combination of spectrograph (Acton 150 with 300 g/mm grating) and back-illuminated CCD cameras (Princeton Instruments, LN 130).

For fluorescence lifetime measurements, a cavity-dumped dye laser (Coherent 700) operating with Rhodamine 6G pumped by a mode-locked YAG:Nd laser (Coherent Antares) was used. The output of the dye laser was at 592 nm with a 10 ps pulse width and 5.4 MHz repetition rate. A fraction of the laser power was delivered through a single-mode optical fiber to the single-molecule imaging system. Single-molecule fluorescence lifetimes were measured by time-correlated photon counting with an instrumental response time of 180 ps.[15]

Fluorescence intensity trajectories were recorded with continuous-wave (CW) excitation at 594 nm by a helium−neon laser (Research Electrooptics), as well as at 568 nm by the Kr line and at 592 nm by the pulsed dye laser. Polarization modulation experiments were done by continuously rotating a half-wave plate in the excitation beam at a rate of 20 Hz.

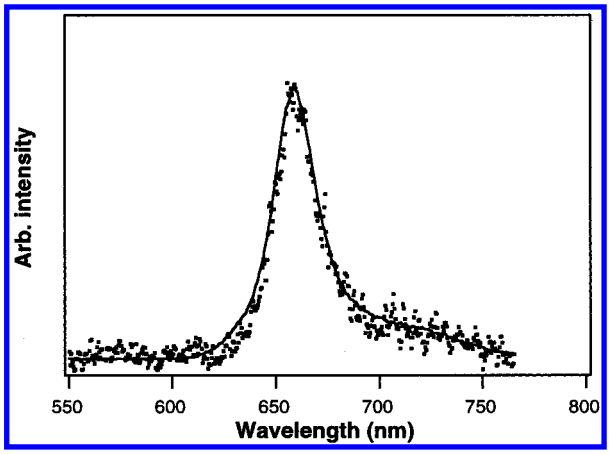

Figure 3. Comparison of the fluorescence spectrum of a single allophycocyanin trimer with the ensemble spectrum. (···) Single molecule spectrum; (—) ensemble-averaged spectrum. Most single-molecule spectra are the same as ensemble spectra within the experimental error. The excitation wavelength was 568 nm, and excitation power at the sample was 700 nW.

Results

Fluorescence Spectra. Figure 3 shows the fluorescence spectrum of a single APC trimer that is identical to the ensemble spectrum. The data collection time was 1 s. Among the 200 molecules we studied, 98% gave identical spectra within experimental error. The shape and peak positions for most molecules did not change with time before photobleaching, even though the intensity of the spectra varied substantially and on−off blinking was observed (see below). This result indicates that the single APC trimer spectrum is homogeneous on the time scale of the measurements.

The fluorescence peaks of 30% of the molecules changed from 659 to 640 nm just before photobleaching. The emission maximum of the APC monomer is at 640 nm.[21] We attribute the blue-shifted emission to the last unbleached α84 or β84 chromophore. There is a significant intensity reduction (down to 10%) associated with the spectral blue shift. Unfortunately, measurements on single APC monomers prepared from dilute solution of non-cross-linked APC trimers are generally difficult because the monomers undergo very fast photobleaching.

For APC trimers dried on glass surfaces and APC trimers imbedded in poly(methyl methacrylate) film, a broad distribution of spectral means as well as spectral fluctuations were observed, similar to dye molecules in a polymer matrix.[14] The aqueous environment sped up the fluctuations.

Fluorescence Intensity Trajectories. Fluorescence intensity trajectories of single APC trimers were measured at different excitation conditions with CW circular polarized light. Figure 4a shows the fluorescence trajectory of an APC trimer taken with 250 nW of excitation power at 594 nm. Three intensity levels can be clearly identified. Figure 4b shows another trajectory taken with 500 nW excitation light at 568 nm. It is noteworthy that reversible jumps occur between different intensity levels before the final photobleaching. Considering that there is no spectral fluctuation at the same time scale, we attribute the highest intensity level to three emitting pairs of strongly coupled α84 and β84, the intermediate intensity level to two emitting pairs, and the lowest intensity level to only one emitting pair. Photoinduced effects create exciton traps within the strongly coupled α84 and β84 pairs, which substantially quench the emission within a pair so that the total emission vanishes in pairs. This assignment will be further proved by a polarization modulation experiment described below. We found

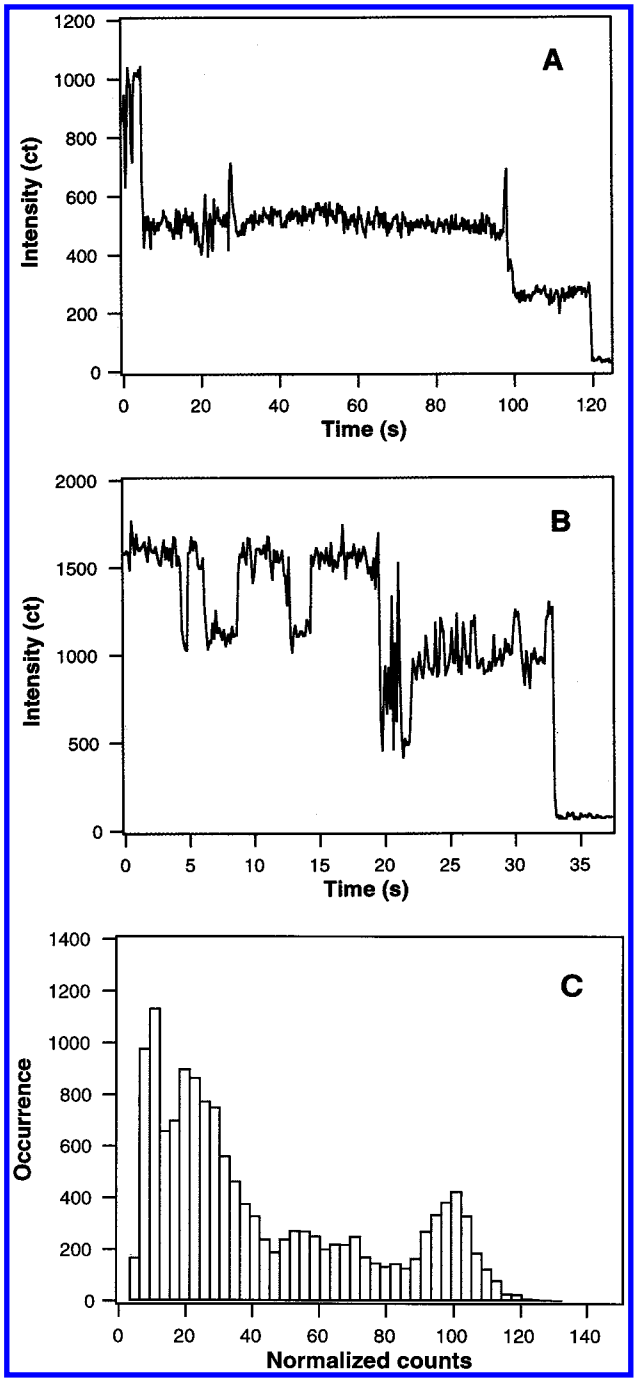

Figure 4. (A) Fluorescence intensity trajectory of a single allophycocyanin trimer showing the sequential bleaching of the three chromophore pairs. The time bin was 125 ms. (B) Another fluorescence intensity trajectory with excitation wavelength at 594 nm and time bin of 125 ms. (C) Combined intensity histogram of 41 individual molecules. Each trajectory was normalized to its initial intensity. The first peak is the background level. The other three peaks represent the fluorescence from one, two, and three pairs.

90% of the molecules show similar multistep behavior. Following ref 18, we show a normalized intensity histogram (Figure 4c) for 41 individual molecules. In addition to the weakest peak corresponding to the background signal, there are three distinct intensity levels. The ratio of the three peak intensities (background-subtracted) in the histogram are 6:3:1 (instead of 3:2:1) because of quenching of the fluorescence by the exciton trap(s) in the adjacent pair(s), as evidenced by the lifetime measurements described below. The spreads of the three peaks in the histogram are due to heterogeneity of APC properties,

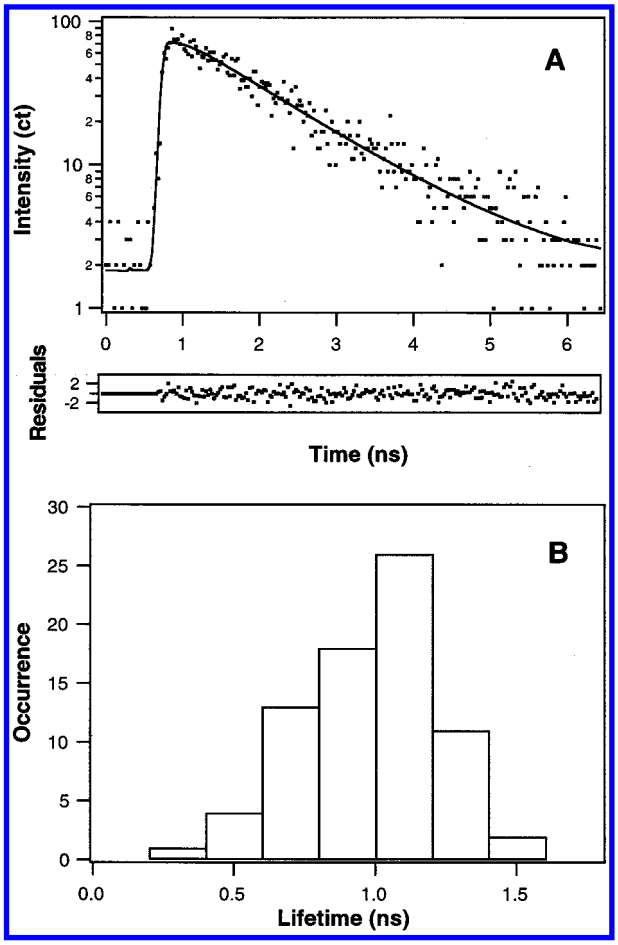

Figure 5. (A) Fluorescence decay of a single allophycocyanin trimer immobilized on cover glass. The solid line is a single-exponential fit ($t = 1.24$ ns, $\chi^2 = 0.98$) with the instrumental response function (fwhm 180 ps). (B) Histogram of fluorescence lifetimes for 75 individual molecules.

such as the relative orientation of an APC trimer to the surface. We note that not every molecule undergoes the sequential intensity jumps. For instance, in Figure 4B, intensity can jump (at the 19th second) from the three-pair level to the one-pair level due to insufficient time resolution, but the probability of this kind of jump is relatively small.

Fluorescence Lifetimes. Figure 5a shows the fluorescence decay of a single APC trimer lifetime fitted by a single exponential decay. In contrast to the homogeneous spectra, an extremely broad lifetime distribution for individual APC trimers is observed with an average value around 1 ns (Figure 5b). Ensemble-averaged measurements, on the other hand, showed a double-exponential decay. One time constant is 1.51 ns with a weight of 68%, and the other is 0.63 ns with a weight of 32%. It is surprising that the lifetimes measured in single-molecule experiments are often shorter than the ensemble-averaged lifetime. This is caused by the higher excitation rate associated with the single-molecule measurements, which results in exciton traps quenching the emission.

We also measured the fluorescence lifetimes of single APC monomers prepared from a dilute solution of non-cross-linked APC trimers. APC monomers have significantly shorter lifetimes than APC trimers, as well as a broader distribution of lifetimes, which can be attributable to the flexible tetrapyrrole chains after the disruption of the trimer structure.

Figure 6 shows simultaneous lifetime and intensity trajectories for two APC trimers. The time bin was 0.5 s, and the lifetime

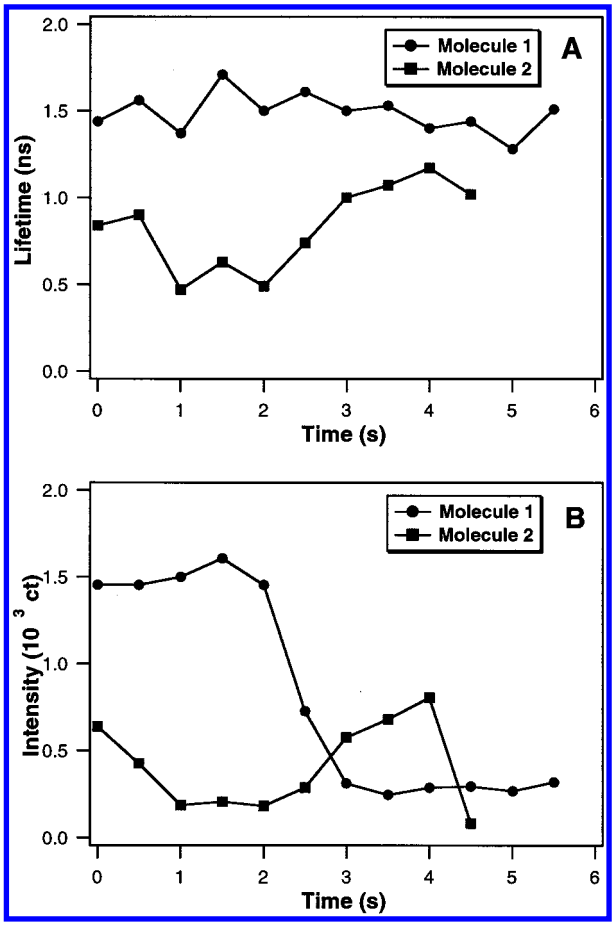

Figure 6. Fluorescence lifetime (A) and intensity (B) trajectories for two APC molecules with binning time of 0.5 s. Lifetimes were obtained fitting with a single exponential. (●) Lifetime and intensity of a molecule are uncorrelated, indicating photobleaching of independent pair(s). (■) Lifetime and intensity of another molecule are correlated, indicating the existence of an exciton trap.

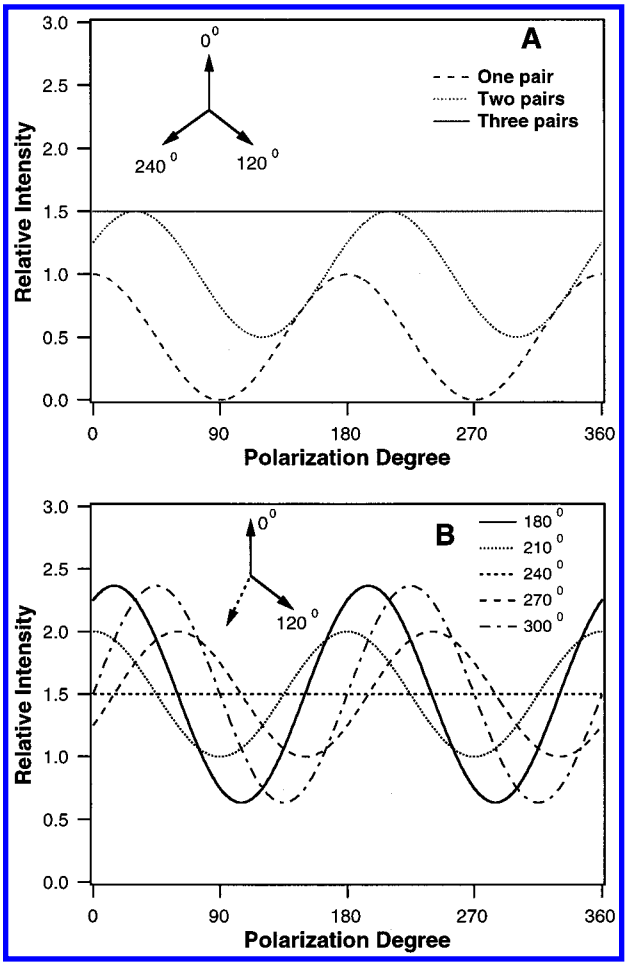

Figure 7. (A) Calculated polarization modulation traces for one, two, and three pairs. The disk-like APC trimer is assumed to be laid-down flat on a flat sample surface. The polarization direction of the excitation light is rotated within the sample plane. (B) Calculated polarization modulation traces for two pairs plus a single unpaired chromorphore with the transition dipole at various angles.

trajectories were recorded with no deadtime. The data fitting was done by convoluting a single exponential with an instrumental response (full width of half-maximum of 180 ps). Because of the low number of counts per time bin, we did not attempt to fit the data with double-exponential decays. The objective was not to obtain accurate lifetimes for the single molecules, but to evaluate the correlation between lifetime and intensity variations.

Both correlated and uncorrelated behaviors were observed. For molecule1 (dotted curves), the lifetime (Figure 6A) was unchanged as the intensity was reduced from the three- to one-pair level, indicating quasi-independent pairs. In contrast, as the intensity of molecule 2 changed from the level of two pairs to one pair, the lifetime shortened, indicating additional quenching by the extinguished pair. The two behaviors arise from two distinctly different mechanisms, photobleaching and trap formation, respectively.

We found that single APC trimers bleach much faster with pulsed excitation than with CW excitation, so all the single-molecule lifetimes were measured at a lower excitation power of 200 nW.

Polarization Modulation. Polarization modulation of the excitation light can yield detailed information on the orientation of the transition dipoles. According to the C_3 symmetry of the trimer,[22] the fluorescence intensity can be regarded as the incoherent summation of emission from three quasi-independent chromophore pairs. Assuming the disklike APC trimer is laid-down flat on the glass surface, fluorescence intensity induced by excitation to the higher exciton band can be written as

$$I = P\sigma_1\eta_1 \cos^2(\omega t + \theta) + P\sigma_2\eta_2 \cos^2\left(\omega t + \theta + \frac{2}{3}\pi\right) + P\sigma_3\eta_3 \cos^2\left(\omega t + \theta + \frac{4}{3}\pi\right) \quad (1)$$

where P is the laser power density; σ_1, σ_2, and σ_3 are the absorption cross-sections of the lower exciton band at the excitation wavelength; η_1, η_2, and η_3 are the fluorescence quantum yields of the three pairs; ω is the frequency of polarization modulation; and θ is the initial phase. Figure 7a shows a calculation of the emission intensity influenced by polarization modulation for an APC trimer laid-down flat on a substrate. For three identical pairs (inset of Figure 7a), $\sigma_1 = \sigma_2 = \sigma_3 = \sigma$ and $\eta_1 = \eta_2 = \eta_3 = \eta$, eq 1 can be simplified as

$$I = P\sigma\eta(\cos^2(\omega t + \theta) + \cos^2(\omega t + \theta + 2/3\pi) + \cos^2(\omega t + \theta + 4/3\pi)) = 1.5\, P\sigma\eta \quad (2)$$

Therefore, no modulation of the fluorescence intensity should be seen (solid line in Figure 7A). After the formation of an exciton trap in one of the three pairs ($\eta_3 = 0$, for example), a

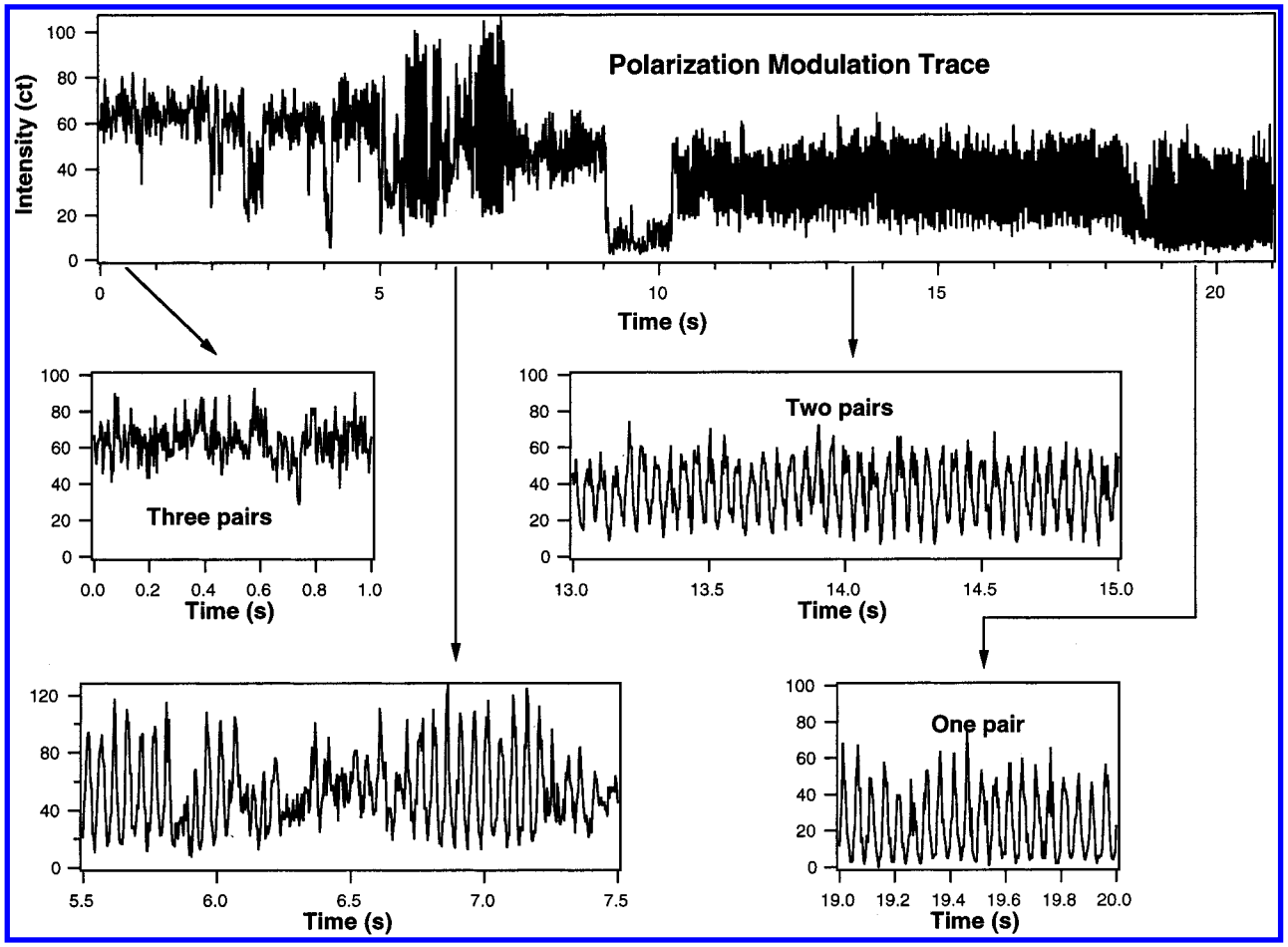

Figure 8. Experimentally measured polarization modulation trace. The zoomed-in portions show that the three pairs are all emitting (0.0−1.0 s) initially, then two pairs emitting (13.0−15.0 s), and finally only one pair emitting (19.0−20.0 s), similar to the calculated traces in Figure 7A. The portion between 5.5 and 7.5 s indicates two pairs plus a single unpaired chromorphore emitting, similar to the calculation in Figure 7B.

moderate modulation should be seen (dotted line in Figure 7A, assuming the trap does not quench the emission of the adjacent pairs, i.e., $\eta_1 = \eta_2 = \eta$). When emission from two pairs are gone because of either trap formation or photobleaching, emission from the remaining pair results in a 100% modulation (dashed line in Figure 7A).

It is important to distinguish trap formation from photobleaching. Trap formation results in the one-step disappearance of emission within a pair caused by formation of an absorbing radical cation, which substantially (but not completely) quenches the emission of the other chromophore in the pair. Photobleaching is caused by irreversible excited-state photochemical reactions, such as photooxidation or hydrogen abstraction,[1,37] generating nonabsorbing species. Two-step sequential photobleaching has been observed in a relatively weakly coupled donor−acceptor system.[12] As will be seen below, we observed that two-step photobleaching still occurs in the strongly coupled α84 and β84 pairs in APC trimers, although it is dominated by the one-step trap formation. The trap formation is approximately three times more probable than the bleaching.

In contrast to the pairwise extinction due to the trap formation, Figure 7B shows the simulation of a polarization modulation trace for an APC trimer with only an α84 (or β84) within one of the three pairs photobleached. Even with the crystal structure, it is difficult to determine the angle of the transition dipole moments of α84 (or β84). A variety of angles with respect to the higher energy exciton dipole are simulated. We assume that the absorption cross section for the α84 (or β84) chromophore is the same as the higher energy exciton band of the pair, which is a reasonable assumption based on the absorption cross sections of α84 (β84) and the two excitonic states. A significant modulation is present in Figure 7B, unless the transition dipole of α84 (or β84) is parallel with that of the higher exciton band (240° case).

An experimentally measured polarization modulation trace is shown in Figure 8. The zoomed-in figures for time periods 0−1.0, 13.0−15.0, and 19.0−20.0 s correspond to three-pair, two-pair, and one-pair states, respectively, with their averaged level and modulation depth consistent to the simulations in Figure 7A. The time period between 5.5 and 7.5 s corresponds to reversible bleaching of α84 (or β84) within a pair, similar to the simulations in Figure 7B.

Figure 9 shows another interesting polarization modulation trace. Photodamage to the trimer is already apparent at the onset of the trajectory recording. The modulation curves are fit by a sine wave. The two bright states (0−1.0 and 2.4−3.1 s) have the same phases, indicating the same emitting species, possibly the two emitting pair (dotted line Figure 7A) or two emitting pair plus an unbleached α84 (or β84) (Figure 7B) states. The two dim states (1.1−2.3 and 3.4−3.6 s) have 100% modulation, corresponding to emission from single emitting pairs (dashed line Figure 7A). The phase difference between them is 128° ± 10°, close to 120°, indicating an alternation between two emitting single pairs for the two dim states, which is consistent with the C_3 symmetry of APC trimer.

Comparison of CW Excitation with Pulsed Excitation. Figure 10 shows the intensity trajectories of two APC trimers taken with continuous excitation (panel A) and a picosecond

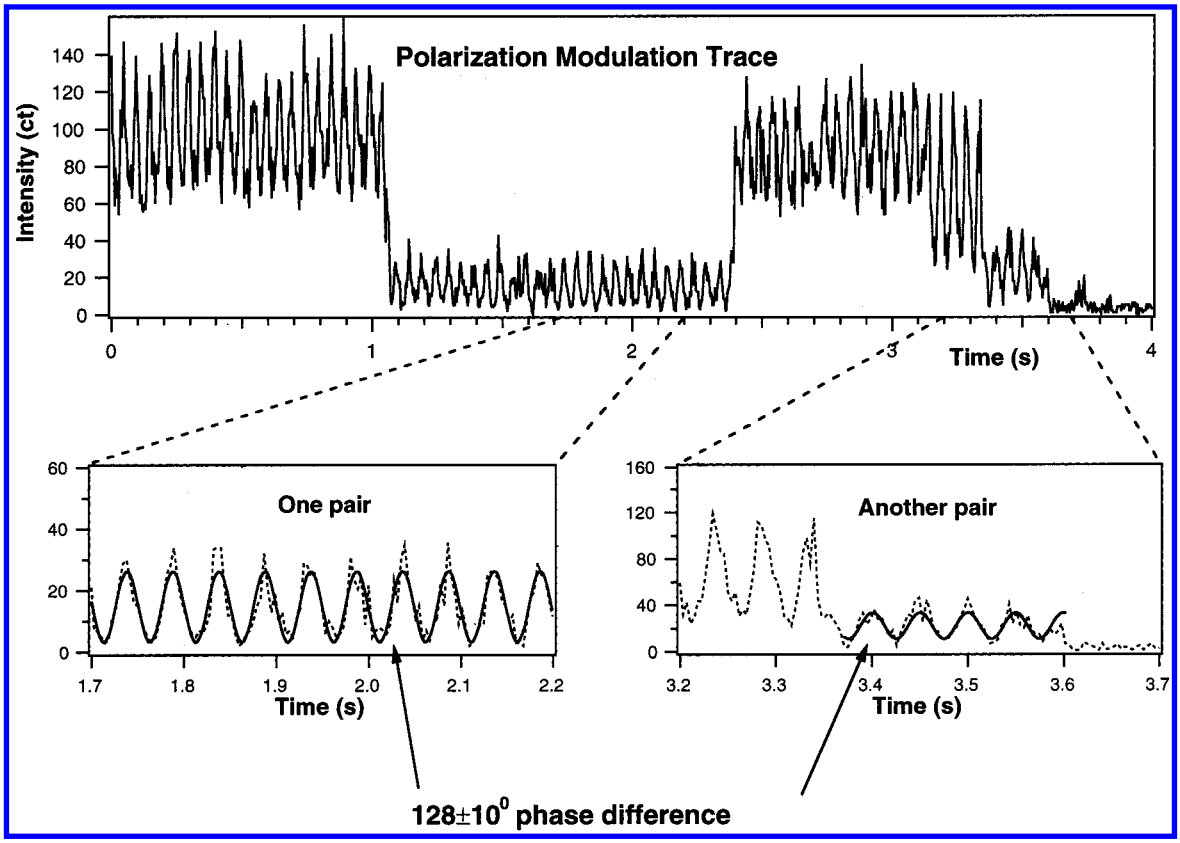

Figure 9. Another experimental modulation trace showing the formation of exciton traps. The two bright states have the same phase, indicating the same emitting species (two pairs). The two dim states correspond to two single emitting pairs. The second dim state has a phase shift of 128° (close to 120°) to the first dim state, indicating a switching between the emitting pairs.

pulse train (panel B) with identical average power, at essentially the same wavelengths, 592 and 594 nm, respectively. The significantly shorter trajectory with the picosecond pulse excitation is evident, indicating a multiphoton mechanism for photobleaching.

Figure 11A,B shows the corresponding histograms of the emitted photon numbers and dwell time (insets) of the first bright state for 56 molecules. From exponential fits to these distributions, the average survival times for the initial bright state are derived to be 10.4 and 0.66 s for the CW and pulsed excitation, respectively, with corresponding averaged emitted photons of 7.2×10^5 and 3.5×10^4, respectively. Figure 12A,B shows the histograms of total emitted photon numbers before photobleaching of the entire APC trimer. The average total number of emitted photons are 2.6×10^6 and 1.2×10^5 for the CW and pulsed excitation, respectively.

Discussion

Homogeneity of Emission Spectra and Heterogeneity of Lifetimes. It has been established that emission spectra of single-dye molecules immobilized on dry surfaces or in polymer matrixes fluctuate at a rather long time scale under ambient conditions.[14,34,38] For sulforhodamine 101 there are two components in the autocorrelation function of the spectral mean, with time constants of subsecond and tens of seconds, respectively.[14] The faster fluctuation is caused by spontaneous spectral diffusion, while the slow fluctuation is predominantly the result of photodriven effects through excited-state relaxation. The emission spectrum of single APC trimer under buffer solution is the same as that of the ensemble sample, indicating that the dynamics occur on a faster time scale than the time scale of the measurement. It is important to note that the time scale of the dynamics that single-molecule experiments can probe is rather long (>milliseconds). Of course, spectral homogeneity is dependent on the time scale. Three-pulse photon-echo peak-shift measurements on a light-harvesting complex, B820 subunit of LH1 of *Rhodospirillun rubrum*, have clearly shown spectral diffusion on the femtosecond time scale, as well as spectral heterogeneity being "static" on the femtosecond time scale.[39] Recently a similar experiment has been carried out on APC trimers, indicating that spectral diffusion occurs on the 50 fs time scale and is essentially complete within 1 ps,[40] which is consistent with our single-molecule result.

The distribution of fluorescence lifetimes has been determined by single-molecule measurements for a few systems. The lifetime distribution can either be static[15] or dynamic.[41−43] In particular, conformational changes of the protein can vary the environment of a chromophore and thus its lifetime.[41−43] Our examination of the APC monomers shows a broader distribution of lifetimes with an average of 0.9 ns, shorter than those of the trimers. This can be attributed to the fact that the chromophores become more flexible when exposed to the solvent. The APC trimer, on the other hand, has a relatively rigid structure that fixes the chromphores in place. Therefore, our observation of the broad distribution of APC trimers cannot be attributed to conformational variations. The shorter average lifetime of the APC trimers, compared to the ensemble sample, can be explained by formation of long-lived exciton traps that quench the fluorescence. The broad distribution of lifetimes can arise from different types of traps. For example, if a β84 forms a radical cation trap, it can quench the emission from adjacent pairs more efficiently than an α84 trap because of β84's vicinity to the pair (Figure 1A). On the other hand, a photobleached

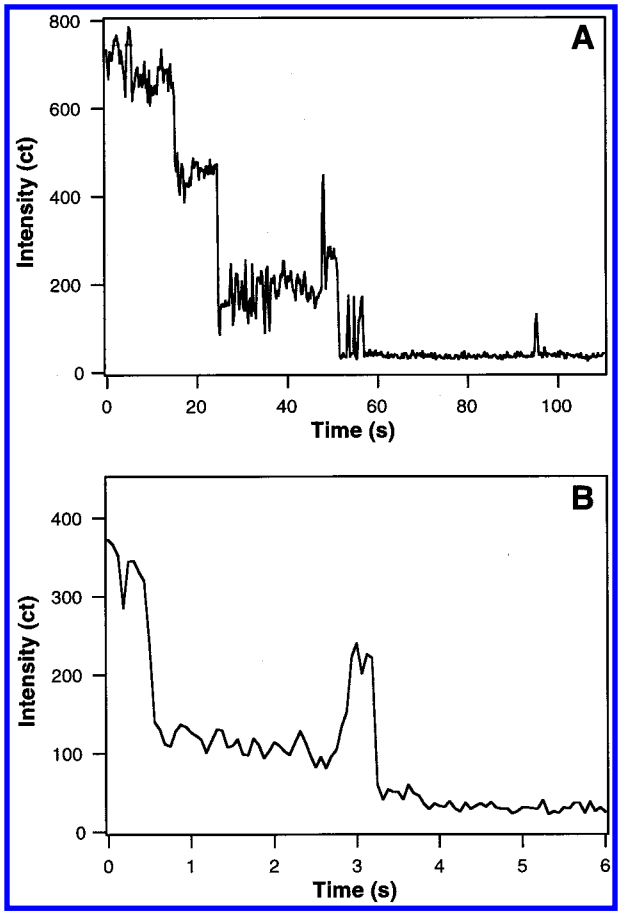

Figure 10. Comparison of emission intensity trajectories taken with (A) CW excitation at 594 nm, 250 nW average power, and 250 ms time bin and (B) picosecond pulse train at 592 nm, 5.4 MHz repetition rate, 250 nW average power, and 62.5 ms time bin.

α84 or β84 does not quench the emission and thus does not alter the other's lifetimes.

Strong Excitonic Coupling Within Pairs. An estimation of the interaction energy of an α84 and a β84 pair in APC trimer gave values of about 110 cm^{-1}, judging from the circular dichroism spectra.[26,44] Therefore, the interaction should be put into the intermediate-to-strong coupling range. Recent experiments done by Beck and co-workers have provided some proof for the strong exciton coupling in the chromophore pairs.[27,28,45] However, the red shift of the absorption maximum of allophycocyanin[29,46] might also result from significant changes in the local environment of α84 or β84 chromophores upon aggregation of three monomers.[22] In this case, the apparent spectral splitting is due to the different spectra of two weakly coupled chromophores.

Our single-molecule experiments lend support to the strongly coupled exciton picture. There are three supporting evidences. First, exciton traps can be the most efficient traps when they form within strongly coupled chromophores. The distinct three- rather than six-step bleaching is indicative of a strongly coupled system. Second, when bleaching of α84 or β84 chromophore occurs (with a low probability) within the last pair, the emission shifts from 659 to 640 nm. 640 nm is the emission maximum of the APC monomer, and the maximum for the α84 or β84 chromophore in an isolated α or β chain.[21] If local environments induced spectral shifts of the α84 and β84 chromophores upon aggregation of three monomers, we would observe a different spectrum for the last unbleached chromophore. The third evidence is a polarization argument that we elaborate as follows.

Assuming that the transition dipole moments for α84 and β84 have the same amplitude, the interaction energy $V_{12} = 220$ cm^{-1} and the angle between the transition dipoles 55° amplitudes of the two exciton bands can be calculated with the standard exciton theory. The two excitonic bands should have their transition dipoles perpendicular to each other (vector sum and vector difference of the α84 and β84 transition dipoles). The absorption spectrum (Figure 1B) of allophycocyanin trimer can be deconvoluted by upper and lower exciton states with center wavelengths of approximately 623 and 654 nm, respectively; the lower state has a width of 470 cm^{-1}, while the upper state has a width of 1700 cm^{-1}.[27] According to the excitonic picture, light at 568 and 592 nm used in our experiments should mainly excite the upper exciton state. The radiationless relaxation down to the lower exciton state occurs on the subpicosecond time scale;[28] thus, the emission is primarily from the lower exciton state. The polarization modulation traces are consistent with the picture of trap formation within the strongly coupled pairs. In contrast, if α84 and β84 are weakly coupled and have two individual absorption band at 623 and 654 nm, excitation of the high-energy chromophore in our experiments will lead to fast Förster transfer to the lower energy band. The lower energy chromophore tends to be bleached first. Bleaching of the lower energy chromophore should not affect the excitation polarization of the higher energy chromophore. Assuming individual α84 and β84 have the same fluorescence quantum yield, the polarization modulation trace (Figure 8) would be unaffected, similar to the simulated situation of 240° (flat) in Figure 7B. Instead, we observed a dramatic modulation upon photobleaching of either α84 or β84, for 5.5−7.5 s in the trace in Figure 8. In other words, a significant change of transition dipole orientation at the excitation wavelength occurred within a single pair. This cannot be readily accounted for by the weakly interacting α84 or β84, but can be attributed to the transition dipole rotating from the orientation of the higher energy exciton band to the unbleached chromophore. Our results are consistent with the fact that allophycocyanin trimer can be regarded as three strongly excitonically coupled pairs with weak coupling among the pairs.

Weak Coupling Among Pairs. Excitonic coupling between two chromophores in different pairs of an APC trimer falls in the weak coupling regime. On the basis of the crystal structure, the Förster energy-transfer rate between an α84 and a β84 in different pairs is estimated to be 1.1 ns^{-1} and between two β84 in different pairs 0.8 ns^{-1}.[22] Therefore, significant energy transfer among the three pairs occurs through the incoherent mechanism within the fluorescence lifetime. If an α84 (or a β84) is photobleached, the β84 (or the α84) within the same pair has a spectrum blue-shifted with respect to the low-energy exciton band. Consequently, the energy-transfer rate between the β84 (or the α84) and another pair is reduced. If an α84 (or a β84) becomes a radical cation quenching the β84 (or the α84) within the same pair, energy transfer to this pair will lead to a shorter fluorescence lifetime of the complex, which we observed experimentally. The rate of Förster energy transfer to the trapping pair is determined by the absorption spectrum of the radical cation trap and the blue-shifted β84 (or the α84) and is expected to be smaller than that among undamaged pairs. This explains the small reduction in the fluorescence lifetime and intensity of the entire complex upon trap formation.

Photochemistry. The repetitive excitation in a single-molecule experiment results in photodamage. Single-chromophore experiments usually involve two mechanisms. First, a chromophore in the long-lived triplet state reacts with triplet

molecular oxygen generating highly reactive singlet oxygen.[47]

$$S_0 \xrightarrow{h\nu} S_1 \rightarrow T_1 \xrightarrow{^3O_2} S_0 + {}^1O_2 \rightarrow \text{bleached} \qquad (3)$$

Second, triplet−triplet absorption, which results in a highly reactive excited state, has been proposed in explaining single-molecule experiments with two-photon excitation.[37,48]

$$S_0 \xrightarrow{h\nu} S_1 \rightarrow T_1 \xrightarrow{h\nu} T_n \rightarrow \text{bleached} \qquad (4)$$

A major objective of this work is to elucidate mechanisms for photodamage of multichromophore systems. The dramatic difference in photostability for CW and pulse excitation at the identical wavelength and average power level indicates a multiphoton effect.

We propose a multiphoton mechanism involving singlet−singlet exciton annihilation for the trap formation and photobleaching, which is operative under picosecond pulse excitation.

$$S_0 \xrightarrow{h\nu} S_1 \quad + \quad S_0 \xrightarrow{h\nu} S_1 \longrightarrow S_n \longrightarrow \text{bleached or trap formed} \qquad (5)$$

Singlet−singlet exciton annihilation is commonly seen in photosynthetic light-harvesting systems excited with highly intense laser pulses.[49] Previous ensemble-averaged measurements showed that the fluorescence lifetime of allophycocyanin trimers is reduced by singlet−singlet annihilation at intensities close to 10^{16} photons pulse^{-1} cm^{-2}.[50] The 250 nW excitation power used in our experiment corresponds to the laser influence of about 2×10^{13} photons pulse^{-1} cm^{-2}, well below the singlet−singlet annihilation threshold, and the probability of a double excitation within one pulse is 2×10^{-3}. Therefore, on average, 500 pulses are needed for a single molecule to get doubly excited. An even larger number of pulses are needed to detect an event via eq 5. This is consistent with our observations.

For CW excitation, it is possible that the processes proceed predominately through a linear mechanism (e.g., photoinduced electron transfer) as suggested by other workers for other systems:[17,18]

$$S_0 \xrightarrow{h\nu} S_1 \rightarrow \text{bleached or trap formed} \qquad (6)$$

However, we have made an observation indicating a multiphoton mechanism, even in the case of CW excitation. Comparing the average number of photons emitted prior to the extinction of the first α84 and β84 pair (7.2×10^5, Figure 11A) and that prior to the complete photobleaching of all three pairs (2.6×10^6, Figure 12A), we found their ratio is 1:(3.6 ± 0.5) rather than 1:3. One would expect a 1:3 ratio based on the linear mechanism (eq 6). Note that the 1:3 ratio is expected even when the trap in the first extinguished pair can quench the emission from the other pairs. This is because the number of photons detected prior to photobleaching is only determined by the ratio of the radiative rate and the bleaching/trap formation rate. In contrast to the expectation from a linear mechanism, our data showed that the larger the number of chromophores, the sooner the photodamage happens. This size-dependent bleaching lifetime indicates an exciton−exciton annihilation mechanism under CW excitation.

If the trap formation and/or bleaching occurred via the singlet−singlet annihilation mechanism (eq 5), the photodamage of CW excitation would be much slower than we observed

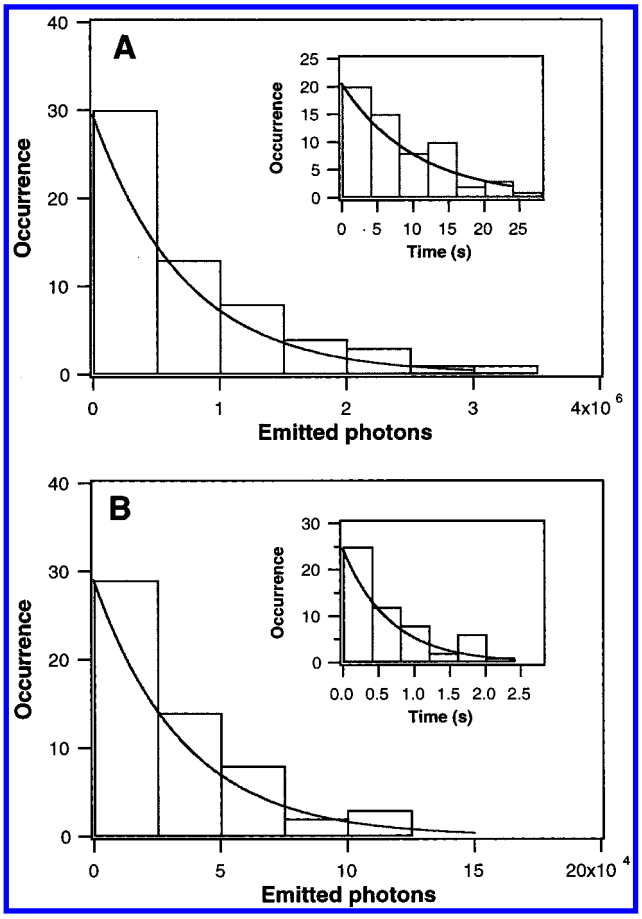

Figure 11. Histograms of the emitted photons from the first bright state of APC trimers under CW (A) and pulsed excitation (B). The insets show histograms of the survival time for the first bright state. The numbers for detected photons were converted to the numbers of emitted photons by assuming a total detection efficiency of 7%. The distributions were fitted by single-exponential decays. The average emitted photons for the CW and the pulsed excitation are 7.2×10^5 and 3.5×10^4, respectively. The average survival time for the first bright state is 10.4 and 0.66 s for CW and the pulsed excitation, respectively.

(Figure 10). The fact that the CW damage rate is only slower than the pulsed damage rate by a factor of 10 suggests that the damage occurs via a different mechanism. We, therefore, propose a multiphoton mechanism involving the singlet−triplet exciton annihilation:[48]

$$S_0 \xrightarrow{h\nu} S_1 \quad + \quad S_0 \xrightarrow{h\nu} T_1 \longrightarrow S_n \longrightarrow \text{bleached or trap formed} \qquad (7)$$

The mechanism can operate under CW excitation conditions for the trap formation and photobleaching in addition to the linear mechanism. This mechanism arises from the frequent visits to the triplet state in the single-molecule measurement.

While the singlet−triplet exciton annihilation mechanism is likely to operate for the CW case, it cannot solely account for the experiment with picosecond pulse excitation because there are many laser pulses (5 MHz repetition rate) during the triplet lifetime. Singlet−singlet annihilation is still needed to explain

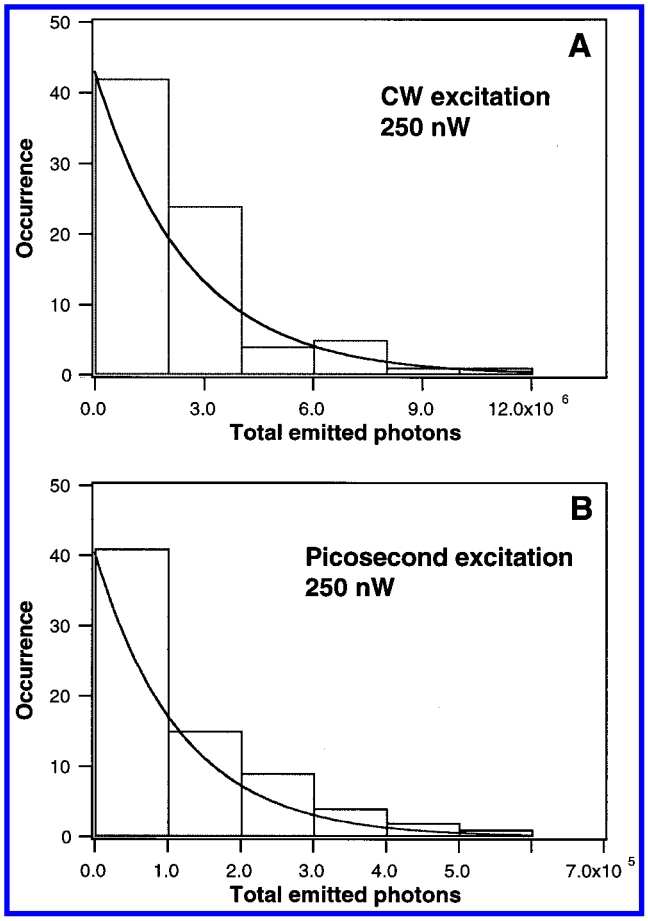

Figure 12. Histograms of total emitted photons before photobleaching for APC trimers under CW (A) and the pulsed excitation (B). The average numbers of total emitted photons for the CW and the pulsed excitation are 2.6×10^6 and 1.2×10^5, respectively.

the dramatic difference between trajectories with CW and picosecond excitation. In other words, bleaching or blinking in the case of pulsed excitation is predominantly due to singlet−singlet annihilation.

We note that previous single-molecule studies of molecular aggregates[17,18] have shown linear intensity dependence of the blinking and bleaching times for both CW[18] and picosecond pulse excitation.[17] In particular, picosecond excitation was used to study LH2 light-harvesting complexes from photosynthetic bacteria. However, the signal-to-noise ratio of the data might not be high enough to exclude quadratic intensity dependence.[17] Comparison of CW and pulse excitation as well as the size-dependent photobleaching lifetime for the APC trimer system suggests that involvement of exciton−exciton annihilation in a single-molecule experiment on molecular aggregates cannot be underestimated.

Details about the chemical nature of the photochemically generated species remain to be determined. We can, however, distinguish at least two distinctly different species: one is the absorbing trap characterized by the pairwise emission disappearance (Figure 4) and the shortened fluorescence lifetimes (Figure 5), which is most likely a radical cation generated by electron transfer. The other is a nonabsorbing or "bleached" species, evidenced with the polarization modulation trace (5.5−7.5 s of Figure 8) and unchanged lifetimes, which is most likely the result of irreversible photooxidation. We note that different mechanisms, linear (eq 6) or nonlinear (eqs 5 and 7), could generate the same species.

It is important to point out that the light-harvesting complexes do not work under such high excitation flux in a natural photosynthetic condition. Trap formation and bleaching dynamics studied here are most relevant to the single-molecule measurements. Nevertheless, these experiments are informative about the excitonic coupling and excited-state dynamics. In particular, these transient spieces were extremely hard to capture with ensemble-averaged measurements because of their extremely low quantum efficiency of formation. Perhaps the most interesting and surprising observation from the single-molecule measurements is that the photochemically generated species, especially the exciton traps, can live for as long as seconds and can spontaneously convert back in the dark. While the implication of this to photosynthesis, if any, is yet to be explored, the generation of photochemical pieces in this manner might be useful from both fundamental and practical standpoints.

Conclusions

Individual APC trimers under ambient conditions have been investigated with fluorescence spectra, lifetimes, intensity trajectories, and polarization modulation. Our results support the picture that an APC trimer can be regarded as three pairs of two excitonic states of the strongly coupled α84 and *β*84 chromophores with much weaker interactions among the pairs. The fluorescence spectra of individual APC trimers are identical to the ensemble-averaged spectrum and are homogeneous on the time scale of seconds. The fluorescence lifetimes, on the other hand, are found to be widely distributed and are shorter than the ensemble-averaged lifetime because of formation of long-lived exciton traps. The exciton traps, most likely radical cations, absorb but do not emit, almost completely quench the emission within an α84 and *β*84 pair, and partially quench the emission from other pairs. In addition to trap formation, there exists photobleaching of individual α84 or *β*84 chromophores, which occurs at a lower probability. The traps and bleached chromophores can be distinguished by polarization modulation traces and the simultaneous fluorescence lifetime and intensity trajectories. The exciton trap formation and/or photobleaching of an individual APC trimer is over an order of magnitude faster for pulse than for CW excitation, indicating nonlinear mechanisms for exciton trap formation and/or photobleaching. Singlet−singlet annihilation is most likely the dominating mechanism under pulsed excitation. The exciton−exciton annihilation exists even under CW excitation, as evidenced by a size-dependent bleaching rate. Singlet−triplet annihilation is most likely the dominating mechanism under CW excitation. The exciton traps are long-lived and spontaneously reversible. Such photochemistry of light-harvesting complexes is difficult to investigate with ensemble-averaged experiments due to extremely low quantum yields for the photochemical species.

Acknowledgment. We thank Cary Johnson and Steve Colson for stimulating discussions and H. Peter Lu, Gary Holtom, and Erik Sanchez for their help with the experiments. We also thank Doug Ray, Alan Joly, and David Laman for the use of their picosecond dye laser system. Pacific Northwest National Laboratory is operated for the U.S. Department of Energy (DOE) by Battelle. This work was funded by the DOE's Office of Energy Research, Chemical Science.

References and Notes

(1) For a recent review, see: Xie, X. S.; Trautman, J. K. *Annu. Rev. Phys. Chem.* **1998**, *49*, 441.

(2) Betzig, E.; Chichester, R. J. *Science* **1993**, *262*, 1422.

(3) Trautman, J. K.; Macklin, J. J.; Brus, L. E.; Betzig, E. *Nature* **1994**, *369*, 40.

(4) Xie, X. S.; Dunn, R. C. *Science* **1994**, *265*, 361.

(5) Ambrose, W. P.; Goodwin, P. M.; Martin, J. C.; Keller, R. A. *Science* **1994**, *265*, 364.
(6) Eigen, M.; Rigler, R. *Proc. Natl. Acad. Sci. U.S.A.* **1994**, *91*, 5740.
(7) Nie, S.; Chiu, D. T.; Zare, R. N. *Science* **1994**, *266*, 1018.
(8) Funatsu, T.; Harada, Y.; Tokunaga, M.; Saito, K.; Yanagida, T. *Nature* **1995**, *374*, 555.
(9) Schmidt, Th.; Schutz, G. J.; Baumgartner, W.; Gruber, H. J.; Schindler, H. *J. Phys. Chem.* **1995**, *99*, 17662.
(10) Xue, Q. F.; Yeung, E. S. *Nature* **1995**, *373*, 681.
(11) Macklin, J. J.; Trautman, J. K.; Harris, T. D.; Brus, L. E. *Science* **1996**, *272*, 255.
(12) Ha, T.; Enderle, T.; Chemla, D. S.; Selvin, P. R.; Weiss, S. *Proc. Natl. Acad. Sci. U.S.A.* **1996**, *93*, 6264.
(13) Vale, R. D.; Funatsu, T.; Pierce, D. W.; Romberg, L.; Harada Y.; Yanagida, T. *Nature* **1996**, *380*, 451.
(14) Lu, H. P.; Xie, X. S. *Nature* **1997**, *385*, 143.
(15) Lu, H. P.; Xie, X. S. *J. Phys. Chem.* **1997**, *101*, 2753.
(16) Dickson, R. M.; Cubitt, A. B.; Tien, R. Y.; Moerner, W. E. *Nature* **1997**, *388*, 355.
(17) Bopp, M. A.; Jia, Y.; Li, L.; Cogdell, R. J.; Hochstrasser, R. M. *Proc. Natl. Acad. Sci. U.S.A.* **1997**, *94*, 10630.
(18) Vanden Bout, D. A.; Yip, W.-T.; Hu, D.; Fu, D.-K.; Swager, T. M.; Barbara, P. F. *Science* **1997**, *277*, 1074.
(19) Wu, M.; Goodwin, P. M.; Ambrose, W. P.; Keller, R. A. *J. Phys. Chem.* **1996**, *100*, 17406.
(20) Yip, W.; Hu, D.; Yu, J.; Vanden Bout, D. A.; Barbara, P. F. *J. Phys. Chem. A* **1998**, *102*, 7564.
(21) MacColl, R.; Guard-Friar D. *Phycobiliproteins*; CRC Press: Boca Raton, FL, 1987.
(22) Brejc, K.; Ficner, R.; Huber, R.; Steinbacher, S. *J. Mol. Biol.* **1995**, *249*, 424.
(23) Davydov, A. S. *Theory of Molecualr Exciton*; Mcgraw-Hill: New York, 1962.
(24) Förster, T. In *Modern Quantum Chemistry*; Sinanoglu, O., Ed.; Academic: New York, 1965; p 93.
(25) MacColl, R.; Csatorday, K.; Berns, D. S.; Traeger, E. *Biochemistry* **1980**, *19*, 2817.
(26) Castorday, K.; MacColl, R.; Csizmadia, V.; Grabowski, J.; Bagyinka, C. *Biochemistry* **1984**, *23*, 6466.
(27) Edington, M. D.; Riter, R. E.; Beck, W. F. *J. Phys. Chem.* **1996**, *100*, 14206.
(28) Edington, M. D.; Riter, R. E.; Beck, W. F. *J. Phys. Chem. B* **1997**, *101*, 4473.
(29) Beck, W. F.; Sauer, K. *J. Phys. Chem.* **1992**, *96*, 4658.
(30) Xie, X.; Du, M.; Mets, L.; Fleming, G. R. *Proceeding of SPIE92, Time-Resolved Laser Spectroscopy in Biochemistry III*, 1992; Vol. 1640, p 690.
(31) Oi, V.; Glazer, A. N.; Stryer, L. *J. Cell Biol.* **1982**, *93*, 981.
(32) Tsien, R. Y.; Waggoner, A. In *Handbook of Biological Confocal Microscopy*; Pawley, J. B., Ed.; Plenum Press: New York, 1995; p 267.
(33) Dunn, R. C.; Allen, E. V.; Joyce, S. A.; Anderson, G. A.; Xie, X. S. *Ultarmicroscopy* **1995**, *57*, 113.
(34) Ha, T.; Enderle, Th.; Chemla, D. S.; Selvin, P. R.; Weiss, S. *Phys. Rev. Lett.* **1996**, *77*, 3979.
(35) Ha, T.; Enderle, Th.; Chemla, D. S.; Weiss, S. *Phys. Rev. Lett.* **1998**, *80*, 2093.
(36) Ong, L. J.; Glazer, A. N. *Physiol. Veg.* **1985**, *23*, 777. Yeh, S. W.; Ong, L. J.; Clark, J. H.; Glazer, A. N. *Cytometry* **1987**, *8*, 91.
(37) Sanchez, E. J.; Novotny, L.; Holtom, G. R.; Xie, X. S. *J. Phys. Chem. A* **1997**, *101*, 7019.
(38) Tietz, C.; Daum, R.; Drabenstedt, A.; Schuster, J.; Fleury, L.; Gruber, A.; Wrachtrup, J.; Vonborczyskowshi, C. *Chem. Phys. Lett*. **1998**, 282, 164.
(39) Yu, J.; Nagasawa, Y.; van Grondelle, R.; Fleming, G. R. *Chem. Phys. Lett.* **1997**, *280*, 404.
(40) Homoelle, B. J.; Edington, M. D.; Diffey, W. M.; Beck, W. F. *J. Phys. Chem.* **1998**, *102*, 3044.
(41) Edman, L.; Mets, Ü., Rigler, R. *Proc. Natl. Acad. Sci. U.S.A.* **1996**, *93*, 6710.
(42) Jia, Y.; Sytnik, A.; Li, L.; Vladimirov, S.; Cooperman, B. S.; Hochstrasser, R. M. *Proc. Natl. Acad. Sci. U.S.A.* **1997**, *94*, 7932.
(43) Geva, E.; Skinner, J. L. *Chem. Phys. Lett.* **1998**, *288*, 225.
(44) Holzwarth, A. R.; Bittersmann, E.; Reuter, W.; Wehrmeyer, W. *Biophys. J.* **1990**, *57*, 133.
(45) Riter, R. E.; Edington, M. D.; Beck, W. F. *J. Phys. Chem. B* **1997**, *101*, 2366.
(46) MacColl, R.; Csatorday, K.; Berns, D. S.; Traeger, E. *Arch. Biochem. Biophys*. **1981**, *208*, 42.
(47) Turro, N. J. *Modern Molecular Photochemistry*; Benjamin/Cummings Publishing: CA, 1978.
(48) Eggeling, C.; Brand, L.; Seidel, C. A. M. *Bioimaging* **1997**, *5*, 105.
(49) van Grondelle, R. *Biochim. Biophys. Acta* **1985**, *811*, 147.
(50) Doukas, A. G.; Stefancic, V.; Buchert, J.; Alfano, R. R.; Zilinskas, B. A. *Photochem. Photobiol.* **1981**, *34*, 505.